Received: 13 October 2020 | Revised: 13 January 2021 | Accepted: 14 January 2021

DOI: 10.1002/jccs.202000456

SPECIAL ISSUE PAPER

JOURNAL OF THE CHINESE CHEMICAL SOCIETY

New carboline-based donors for green exciplex-forming systems

Chia-Hsun Chen[1] | Ju-Ting Cheng[1] | Wen-Cheng Ding[2] | Zong-Liang Lin[1] | Yi-Sheng Chen[1] | Tien-Lung Chiu[3] | Yuan-Chih Lo[1] | Jiun-Haw Lee[2] | Ken-Tsung Wong[1,4]

[1]Department of Chemistry, National Taiwan University, Taipei, Taiwan

[2]Graduate Institute of Photonics and Optoelectronics and Department of Electrical Engineering, National Taiwan University, Taipei, Taiwan

[3]Department of Electrical Engineering, Yuan Ze University, Taoyuan, Taiwan

[4]Institute of Atomic and Molecular Science, Academia Sinica, Taipei, Taiwan

Correspondence
Jiun-Haw Lee, Graduate Institute of Photonics and Optoelectronics and Department of Electrical Engineering, National Taiwan University, Taiwan.
Email: jiunhawlee@ntu.edu.tw
Ken-Tsung Wong, Department of Chemistry, National Taiwan University, Taipei, Taiwan.
Email: kenwong@ntu.edu.tw

Funding information
European Union's Horizon 2020, Grant/Award Number: Marie Skłodowska-Curie grant agreement No 823720; Ministry of Science and Technology, Taiwan, Grant/Award Numbers: MOST 109-2622-E-155-014 : 108-2221-E-155-051-MY3, 107-2221-E-155-058-MY : 107-2113-M-002-019-MY3; Horizon 2020; European Union; Ministry of Science and Technology

Abstract

The carbazole of a model compound CPTBF was replaced by α- and β-carboline to give donors α-CPTBF and β-CPTBF, respectively. The introduction of carboline leads the new donors to have deeper highest occupied molecular orbital (HOMO) energy levels. Different electron acceptors were tested, among them, a new acceptor, 3,4-CN, was found to give exciplexes with efficient green emissions that are blue-shifted as compared to that of model CPTBF:3,4-CN system. The exciplex formations of α-CPTBF:3,4-CN and β-CPTBF:3,4-CN blends were verified with the significantly red-shifted emissions different from those of constituent donor and acceptor together with the delayed fluorescent observed by time-resolved PL decay experiments. The organic light-emitting diode (OLED) devices with α-CPTBF:3,4-CN and β-CPTBF:3,4-CN blends as the emitting layer showed a maximum external quantum (EQE) of 7.57 and 7.34%, respectively, which is higher as compared to that (EQE = 6.87%) of the model device employing CPTBF:3,4-CN. These results were attributed to the higher exciplex photoluminescence quantum yields due to the higher delay fluorescence components, deeper HOMO, and higher triplet energy of the carboline donors. In addition, the β-CPTBF:3,4-CN exciplex-based OLED exhibited better efficiency roll-off at higher luminesce due to more charge balance with less polaron formation, which was analyzed with time-resolved EL.

KEYWORDS

carbazole, carboline, exciplex, organic light-emitting diode, TADF

1 | INTRODUCTION

Organic light-emitting diodes (OLEDs) had attracted lots of attention in display and lighting applications due to the advantages of low weight and high performance as well as the feasibility for flat and flexible large-area substrates.[1,2] The performance of OLED device primarily depends on the photoluminescence quantum yield (PLQY) and the exciton utilization efficiency of the emitters under the electric operation. Thanks to the efforts devoted to the material developments, the 100% of exciton utilization efficiency can be successfully achieved by phosphorescent emitter due to the strong spin-orbit coupling induced by the heavy metal center.[3,4] However, the rarity and thus high cost of the precious metal, mainly iridium, may impede the cost-effective production of OLEDs. The cost

issue could be mitigated by using organic fluorescent emitter with small singlet-triplet splitting (ΔE_{ST}) for giving thermally activated delay fluorescence (TADF). With the sophisticated molecular design that leads the tailor-made molecule to have the separated distributions of the highest occupied molecular orbital (HOMO) and the lowest unoccupied molecular orbital (LUMO) and subtle intramolecular charge transfer, high-efficiency TADF-based OLEDs have been reported.[5–7] The stability issue of TADF emitters due to the relatively slow reverse intersystem crossing (rISC) rate is the current challenge waiting for the future resolutions. In contrast to Frenkel exciton with high exciton binding energy that localizes on one molecule, the exciton formed by intermolecular charge transfer, the so-called "exciplex", at the interface between a donor (D) and an acceptor (A) with sufficiently large energy level off-sets can also give a small exchange energy and thus small ΔE_{ST} for efficient rISC because hole and electron are positioned on D and A, respectively.[8–11] In principle, exciplex-based emitting systems can potentially achieve 100% of internal quantum efficiency (IQE) and high device efficiency.[12,13] The peak wavelength of exciplex emission can be determined by the difference of the HOMO of D and the LUMO of A. Therefore, it is simple to perform color adjustment of exciplex by modifying the molecular energy level of D or A. More importantly, the emitting layer with charge balance and high hole and electron mobilities can be achieved by blending the D and A with good charge carrier transporting characters instead of developing complicated bipolar single host. This can benefit to the low turn-on voltage of exciplex-based OLEDs.[14,15]

To develop an electron donor/acceptor for exciplex without low triplet quenching, high triplet energy moiety such as carbazole[16], carboline[17,18], arylsilane[19], and dibenzofuran[20] are commonly employed. In order to achieve blue-shift emission wavelength of exciplex, electron donor with a deeper HOMO is required. One of the strategies is to decrease the hole density distribution of electron donor, for example, the introduction of an electron-deficient group onto the electron-rich moiety. Carboline moiety, a carbazole derivative with an embedded nitrogen atom within the conjugated aromatic ring, can perform a lower HOMO as compared to that of carbazole. Three carboline derivatives with nitrogen at different positions of pyridoindole unit, α-carboline, β-carboline, and γ-carboline, had been demonstrated as host material by Lee et al. for blue PhOLEDs.[21,22] The triplet energy, HOMO/LUMO level, carrier mobility, and device performances were nicely correlated with the molecular structures.[23] With the capability to control the hole and electron mobility, carboline derivatives were also employed as electron acceptor for exciplex emitting layer.[24]

In this research, we report the synthesis and device application of two novel carboline-based hole-transporting materials, α-CPTBF and β-CPTBF (Figure 1), as electron donor for exciplex-based OLEDs. α-CPTBF and β-CPTBF are modified from a previously reported donor 9,9-bis [4-(carbazol-9-yl)phenyl]-2,7-ditert-butylfluorene (CPTBF) that can perform good exciplex formation with good PLQY and promising device performances due to the remote steric effect.[25] Herein, the carbazole moiety of CPTBF is replaced by α-carboline and β-carboline for giving α-CPTBF and β-CPTBF, respectively, to achieve a deeper HOMO energy level. Therefore, the hypsochromic shift emission of the exciplex that employed α-CPTBF and β-CPTBF as electron donors can be reasonably expected. Different electron acceptors were tested, among them, a new acceptor, 3,4-CN, was found to give exciplexes with efficient green emission. The OLED devices with α-CPTBF:3,4-CN and β-CPTBF:3,4-CN blends as the emitting layer (EML) showed a maximum external quantum (EQE) of 7.57 and 7.34%, respectively, which is higher as compared to that (EQE = 6.87%) of the model device employing CPTBF:3,4-CN blend. The CIE coordinates of the device changed from (0.35, 0.57) for the device with CPTBF:3,4-CN to (0.30, 0.56) and (0.30, 0.56) for the device with α-CPTBF:3,4-CN and β-CPTBF:3,4-CN blend, respectively. These results were attributed to the higher exciplex PLQYs due to the higher contribution of delay fluorescence components, deeper HOMO, and higher triplet energy of the carboline donors. In addition, the β-CPTBF:3,4-CN exciplex-based OLED exhibited better efficiency roll-off at higher luminesce due to more charge balance with less polaron formation, which was analyzed with time-resolved electroluminescence (TrEL).

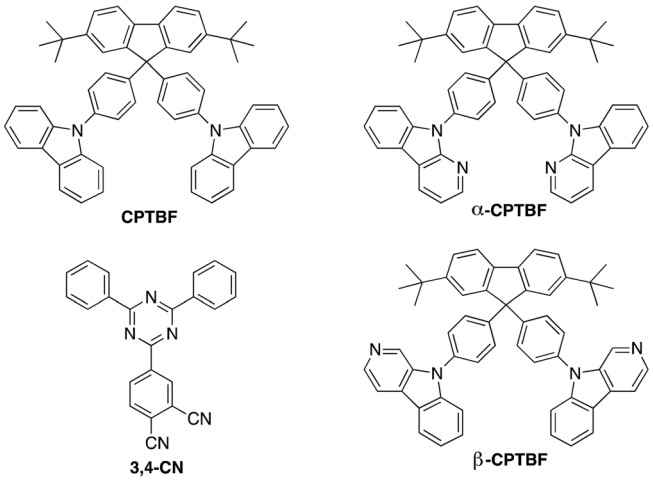

FIGURE 1 Molecular structures of electron donors CPTBF, α-CPTBF, and β-CPTBF and electron acceptor 3,4-CN

2 | RESULTS AND DISCUSSION

The synthesis of the target molecules, α-CPTBF and β-CPTBF, from α-carboline, β-carboline, and fluorene-based compound 1[26] is depicted in Scheme 1. The Cu-catalyzed Ullman reaction of diiodo compound 1 with α-carboline and β-carboline afforded α-CPTBF and β-CPTBF in good yields, respectively. The synthesis of 3,4-CN starts from the boronic acid intermediate 2, which was prepared from 1-bromo-3,4-dichlorobenzene. The Suzuki coupling reaction of 2 and 2-chloro-4, 6-diphenyltriazine gave the product 3, which was further converted to the target compound 3,4-CN via a Pd-catalyzed cyanation reaction with $Zn(CN)_2$. The detailed synthetic procedures and characterizations are included in Supporting Information. The differential scanning calorimetry analysis revealed the glass transition temperature (T_g) of CPTBF, α-CPTBF, and β-CPTBF is 208, 198, and 164°C, respectively. Thermogravimetric analysis was used to analyze the thermal properties of CPTBF, α-CPTBF, and β-CPTBF. In this regard, α-CPTBF and β-CPTBF exhibited better thermal stability with the decomposition temperature (T_d, 5% wt loss) of 362 and 405°C, respectively, which is higher than CPTBF (T_d = 360°C). The new acceptor 3,4-CN also exhibits sufficient thermal stability (T_d = 268°C) for the thermal process. From the density functional theory calculations, which were carried out at m06-2x/6-31G(d) level, the optimized conformations and the populations of HOMO and LUMO of CPTBF, α-CPTBF, and β-CPTBF were analyzed as shown in Figure S1. For α-CPTBF and β-CPTBF, the population of LUMO is localized at the carboline moiety, while the LUMO of CPTBF is localized at the fluorene bridge. Interestingly, the HOMO of α-CPTBF is populated over the whole molecular skeleton, while the HOMO of β-CPTBF and CPTBF is mainly localized at the

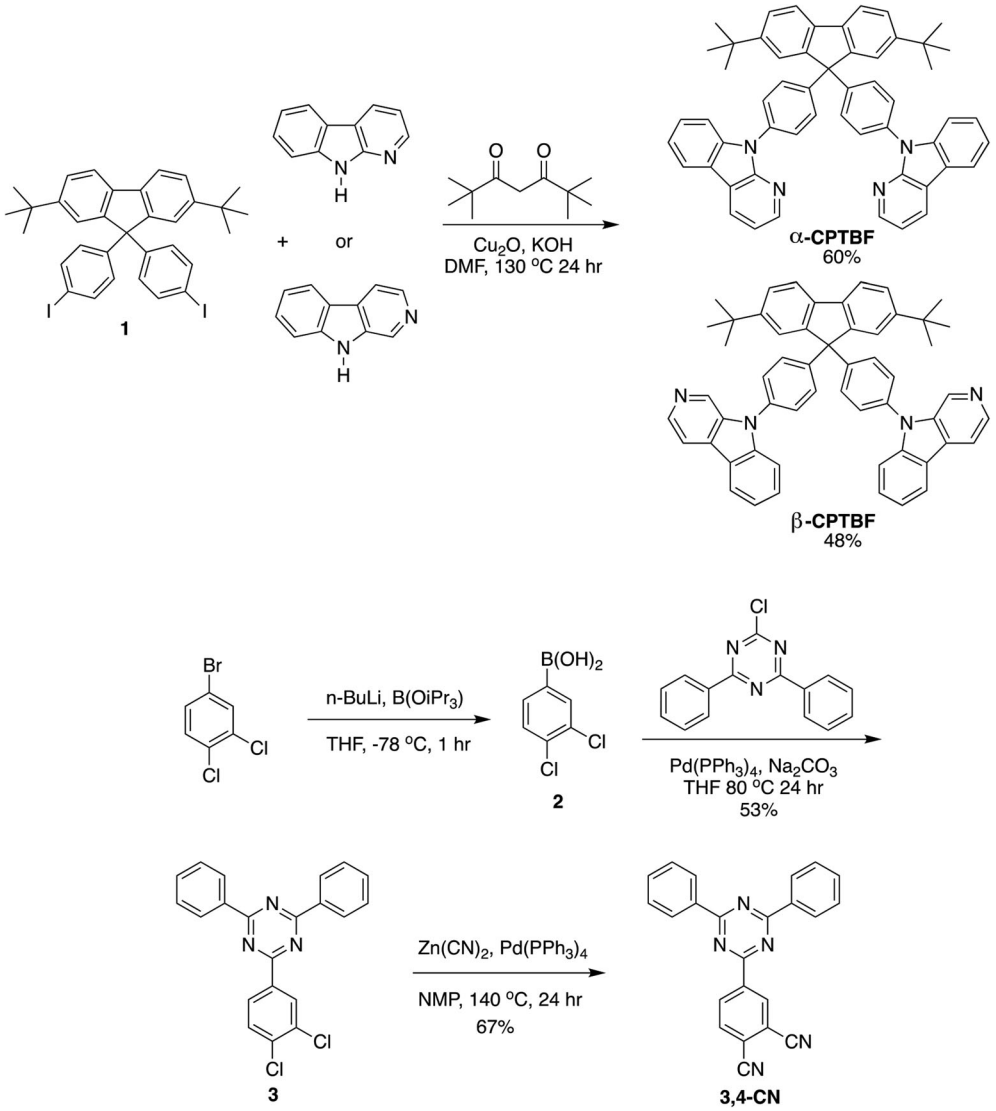

SCHEME 1 Synthesis of α-CPTBF, β-CPTBF, and 3,4-CN

donor and adjacent phenyl groups. Therefore, the structural modification from carbazole to carboline will give rise to the impact more on the LUMO than HOMO.

Figure 2a shows the photophysical properties of CPTBF, α-CPTBF, β-CPTBF, and 3.4-CN in solid neat films, and the data are summarized in Table 1. The absorption bands of CPTBF, α-CPTBF, and β-CPTBF below 300 nm are assigned to the π–π* transitions of the carbazole and carboline. The weak absorption peaks around 310–350 nm are attributed to the n–π* transition of the carbazole and carboline. β-CPTBF shows a slightly stronger absorption peak around 350 nm, which is attributed to the larger oscillator strength according to the theoretical calculation (Table S1). The HOMO obtained from photoelectron spectrophotometer (Figure S2) for CPTBF, α-CPTBF, and β-CPTBF films is −5.86, −5.94, and −5.93 eV, respectively. Agreeing with the theoretical analysis, α-CPTBF and β-CPTBF exhibit deeper HOMO energy levels as compared to that of CPTBF due to the nitrogen substitution on the donor moiety. While the LUMO energy levels (−2.41, −2.70, and −2.63 eV for CPTBF, α-CPTBF, and β-CPTBF, respectively) can be calculated by adding the HOMO energy level and the optical energy gap (E_g) of 3.54, 3.24, and 3.30 eV for CPTBF, α-CPTBF, and β-CPTBF, respectively. Apparently, the descending trend of LUMO levels is more significant than that of HOMO levels due to the introduction of nitrogen atom onto the aromatic ring for giving the stabilization of LUMO orbital. The photoluminescence (PL) emission of α-CPTBF and β-CPTBF films is centered at 375 and 385 nm, respectively, while the emission of CPTBF is centered at 355 and 369 nm. Compared with CPTBF and β-CPTBF, the emission of α-CPTBF is bathochromically shifted by 30 nm, resulting from a stronger resonance effect of the nitrogen atom on the pyridine ring in α-carboline. Calculated from the onset of PL spectra (Figure S3) observed at 77 K, CPTBF, α-CPTBF, and β-CPTBF exhibit high triplet energy as 2.90, 2.90, and 3.08 eV, respectively. The higher triplet level of β-CPTBF can be attributed to the higher triplet energy of β-carboline (2.96 eV) as compared to that of α-carboline (2.89 eV).[21] The main emission peak of 3,4-CN is located at 375 nm. In addition, a longer wavelength emission assigned as the excimer of 3,4-CN centered at 512 nm was observed, indicating the strong intermolecular interactions occurred due to the relative planar molecular structure.

For probing the exciplex formation using CPTBF, α-CPTBF, and β-CPTBF as electron donors, three deep LUMO electron-transporting materials, 1,3,5-triazine-2,4,6-triyl)tris(benzene-3,1-diyl))tris(diphenylphosphine oxide) (PO-T2T), 3′,3‴,3⁗′-(1,3,5-triazine-2,4,6-triyl)tris (([1,1′-biphenyl]-3-carbonitrile)) (CN-T2T), and 3,4-CN

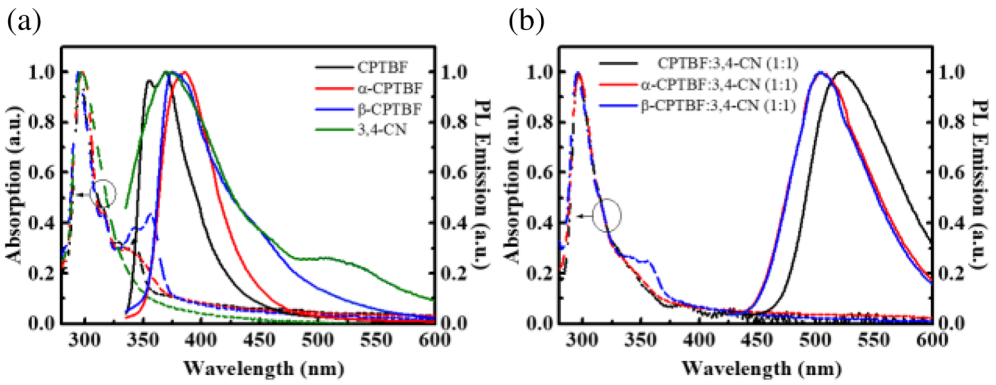

FIGURE 2 Room-temperature absorption and PL spectra of (a) CPTBF, α-CPTBF, β-CPTBF, and 3.4-CN in solid-state neat films. (b) CPTBF: 3,4-CN (volume ratio 1:1), α-CPTBF: 3,4-CN (volume ratio 1:1), and β-CPTBF: 3,4-CN (volume ratio 1:1) in solid-state mixed films

TABLE 1 Photophysical and electrochemical properties of CPTBF, α-CPTBF, and β-CPTBF

Compound	Absorption Sol./ film (nm)[a]	PL emission Sol./ film (nm)[a]	HOMO (eV)[b]	LUMO (eV)[c]	E_g (onset)	ET (eV)[d]	T_g (°C)	T_d (°C)
CPTBF	316, 329, 342/315, 328, 344	357/353, 370	−5.86	−2.41	3.54	2.90	208	360
α-CPTBF	316, 338/316, 338	382/387	−5.94	−2.70	3.24	2.90	198	362
β-CPTBF	332, 345/316, 342, 352	353, 368/375	−5.93	−2.63	3.30	3.08	164	405

[a]Measured in toluene solution (10^{-5} M) and neat films.
[b]Obtained using photoelectron spectrophotometer in neat film. LUMO = HOMO + E_g.
[c]Determined by the onset of the UV–Vis absorption curves in neat film.
[d]Determined by the onset of the phosphorescence.

were selected as electron acceptor candidates.[27,28] These D:A blends were all observed with the significantly red-shifted emissions as compared to the emissions of the constituted donor and acceptor as shown in Figures S4 and S5. However, the residual emission from electron donor and/or acceptor can be observed for the blends with PO-T2T and CN-T2T as electron acceptors, indicating the incomplete exciplex formation. The insufficient energy off-sets between electron donor and acceptors (PO-T2T and CN-T2T) result in the insufficient electron confinement at the D:A interface. In contrast, the blends α-CPTBF:3,4-CN and β-CPTBF:3,4-CN, with new acceptor, exhibit longer wavelength emissions both centered at 504 nm with very weak residual emission as shown in Figure 2b. The lower LUMO energy of 3,4-CN mainly contributes to create a large LUMO energy level off-set that can facilitate the efficient electron transfer from donor to acceptor to generate interfacial excitons upon photoexcitation. Since the absorption spectra of the D:A mixed films are the combination of the constituted molecules in neat film with no additional profile for ground state charge transferred interactions are detected in Figure 2b, and those PL spectra at longer wavelength are attributed to the exciplex emission at the interface. The vibronic patterns within the 330–400 nm are small because the original spectral features of CPTBF, α-CPTBF, and β-CPTBF were overlapped by the structureless pattern from 3, 4-CN. As compared to the exciplex emission (λ_{peak} = 522 nm) of CPTBF:3,4-CN blend, the PL emission of α-CPTBF:3,4-CN and β-CPTBF:3,4-CN blends exhibits ca. 18 nm blue shift. This result fully agrees with the deeper HOMO levels for two carboline-based electron donors.

The photophysical properties of these D:A blends were further probed with time-resolved PL as shown in Figure 3. The presence of delay fluorescence for three mixed films can be clearly observed by monitoring their exciplex emission peak at room temperature. The delay components are originated from the TADF properties of exciplex under optical pumping. By using multi-exponential decay model for fitting the relaxation kinetics, the prompt and delay components as well as their relative contributions to the overall PLQYs are summarized in Table 2. The delayed fluorescence lifetime of the mixed film is slightly shorter from 0.12 μs (CPTBF:3,4-CN) to 0.1 μs (α-CPTBF:3,4-CN) and 0.1 μs (β-CPTBF:3,4-CN). Meanwhile, the contribution of delay components toward overall PLQY also increases from 0.03 (CPTBF:3,4-CN) to 0.45 (α-CPTBF: 3,4-CN) and 0.49 (β-CPTBF: 3,4-CN). These results indicate that carboline-based exciplexes show higher contribution from the ^{3}CT state together with better rISC efficiency for giving higher PLQY of 21% (α-CPTBF:3,4-CN) and 25% (β-CPTBF:3,4-CN) as compared to that (18%) of the model CPTBF:3,4-CN exciplex. It gives reasonable anticipation for better device performances with carboline-based exciplexes serving as EMLs of OLEDs.

The three exciplexes based on the common electron acceptor 3,4-CN as EML for the OLED device configured as ITO/TAPC (50 nm)/mCP (10 nm)/D:3,4-CN (1:1, 20 nm)/ETL (50 nm)/LiF (0.8 nm)/Al were fabricated. 1,1-Bis[(di-4-tolylamino)phenyl]cyclohexane (TAPC) ($\mu_h = 4 \times 10^{-2}$ cm^2/Vs) and 1,3-bis(*N*-carbazolyl)benzene (mCP) layer were applied as hole-transporting and hole injection layer, respectively. For optimizing the device performance, various electron-transporting layers (ETLs) such as CN-T2T, 2,4,6- tris(3-[1H-pyrazol-1-yl]phenyl)-1,3,5-triazine (3P-T2T), PO-T2T, 3,4-CN, and BPhen were tested.[28,29] The summarized results as shown in Figure S6 indicate the superior contribution of PO-T2T to the device characteristics, which might due to better electron mobility ($\mu_e = 4.4 \times 10^{-3}$ cm^2/Vs), electron confinement, hole-blocking ability, and lower refractive index with

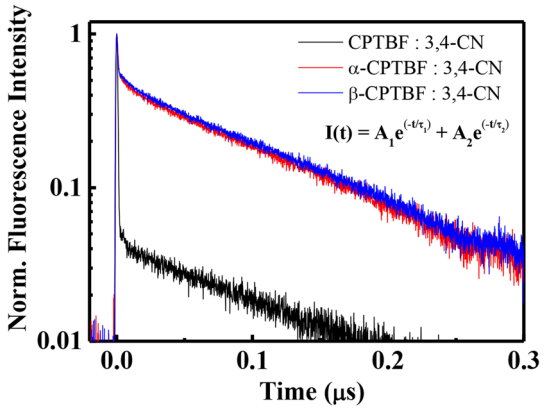

FIGURE 3 Time-resolved PL decay of CPTBF:3,4-CN, α-CPTBF:3,4-CN, and β-CPTBF:3,4-CN mixed films with volume ratio 1:1 in 0.3 μs window at room temperature

Blend	A_1[a]	τ_1 (ns)	A_2	τ_2 (μs)	Φ (%)	Φ_{Prompt} (%)	Φ_{Delay} (%)
CPTBF:3,4-CN	0.96	0.62	0.03	0.12	18	17.4	0.6
α-CPTBF:3,4-CN	0.54	1.34	0.45	0.10	21	11.5	9.5
β-CPTBF:3,4-CN	0.50	1.26	0.49	0.10	25	12.7	12.2

[a]Based on the equation: $I(t) = A_1 \exp(-t/\tau_1) + A_2 \exp(-t/\tau_2)$.

TABLE 2 The fitting results of time-dependent fluorescence decay and PLQYs for CPTBF:3,4-CN, α-CPTBF:3,4-CN, and β-CPTBF:3,4-CN mixed films

higher out-coupling efficiency.[30] Figure 4a–d shows the optimal device performances of three exciplex-based OLEDs, and the data are summarized in Table 3. The devices with α-CPTBF:3,4-CN and β-CPTBF:3,4-CN blends as exciplex EMLs give the improved device efficiency with maximum EQE of 7.57 and 7.34%, respectively, as compared to that (EQE = 6.87%) of the model device employing CPTBF:3,4-CN blend as EML. This can be feasibly attributed to the higher PLQYs of α-CPTBF:3,4-CN and β-CPTBF:3,4-CN mixed films. In addition, the OLED device with β-CPTBF-based exciplex exhibits a lower efficiency roll-off with EQE = 6.68% at 1000 nits. Owing to the deeper HOMO energy levels of carboline-based electron donors, the electroluminescence (EL) emission peaks show blue-shifted from 524 nm (CPTBF:3,4-CN) to 508 nm (α-CPTBF:3,4-CN) and 510 nm (β-CPTBF:3,4-CN) with CIE coordinates changed from (0.35, 0.58) to (0.30, 0.56) and (0.30, 0.56),

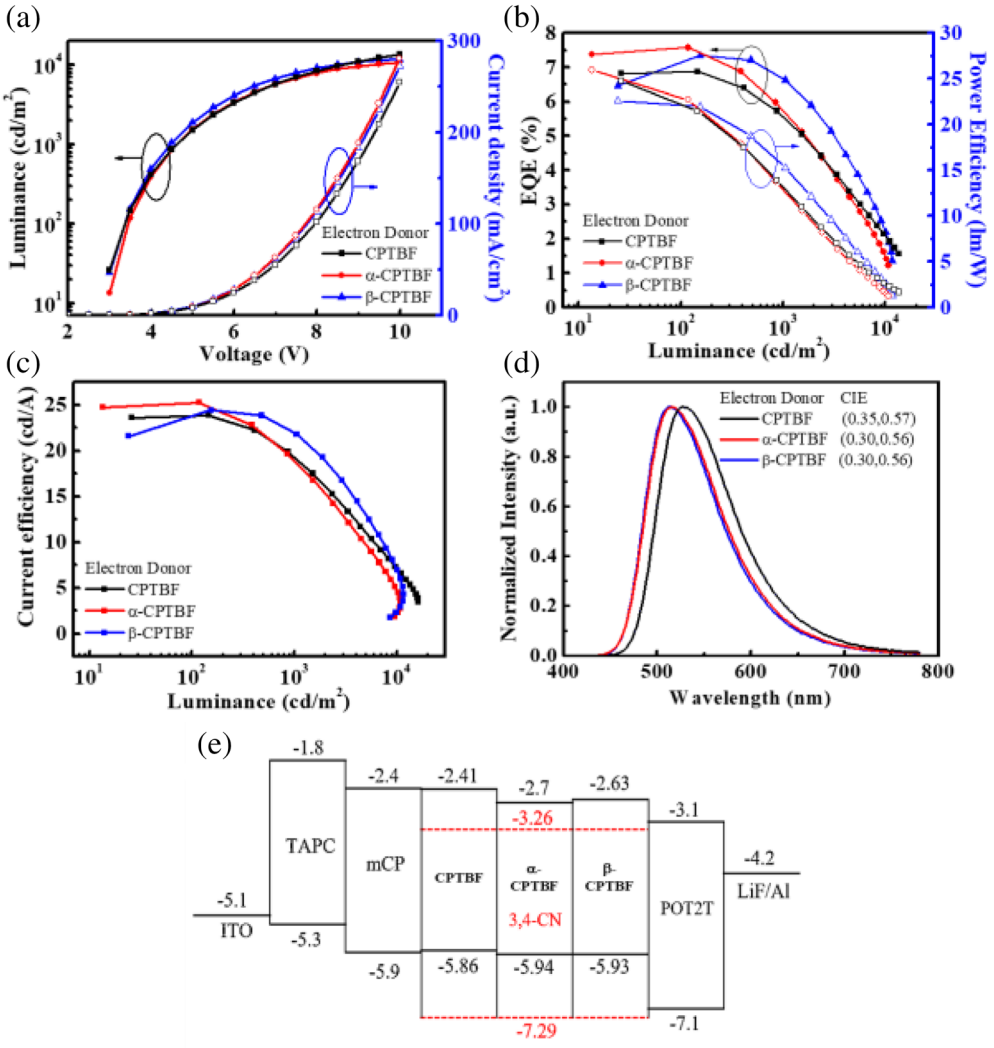

FIGURE 4 (a) Current density–voltage–luminance (J–V–L) characteristics, (b) external quantum (EQE) and power efficiencies (PE) as a function of luminance, (c) current efficiency (CE) as a function of luminance, (d) EL spectra, and (e) device structure of exciplex-based OLEDs

TABLE 3 Devices performances of exciplex-based OLEDs with CPTBF:3,4-CN, α-CPTBF:3,4-CN, and β-CPTBF:3,4-CN blends as emitting layer

EML D:A (volume ratio 1:1)	V at 20 mA/cm²	EQE (%)[a]	η_p (lm/W)[a]	η_c (cd/A)[a]	CIE (x,y)[b]	EL (nm) at 9 V
CPTBF: 3,4-CN	5.74 ± 0.00	6.87 ± 0.01, 5.55	22.6 ± 0.2, 13.1	23.8 ± 0.2, 19.2	(0.35, 0.58)	524
α -CPTBF: 3,4-CN	5.62 ± 0.00	7.57 ± 0.06, 5.73	25.9 ± 0.3, 12.7	25.2 ± 0.3, 18.9	(0.30, 0.56)	508
β-CPTBF: 3,4-CN	5.60 ± 0.00	7.34 ± 0.04, 6.68	24.7 ± 0.2, 15.4	24.4 ± 0.2, 21.9	(0.30, 0.56)	510

[a]Recorded at maximum EQEs, 1,000 cd/m², respectively.
[b]Recorded at maximum EQEs, respectively.

respectively. Furthermore, the current densities of the devices are slightly improved by replacing the fluorene-bridged donor with functional moiety from carbazole to α-carboline and β-carboline. This result might be attributed to better carrier balance, giving the enhancement of maximum power efficiencies (P.E.). Higher power efficiencies with 25.94, 24.75 lm/W are achieved for the α-CPTBF:3,4-CN and β-CPTBF:3,4-CN based OLEDs as compared to the one based on CPTBF:3,4-CN (22.64 lm/W).

Figure S7a–c showed the time-resolved electroluminescence (TrEL) of three exciplex-based OLEDs under different driving voltages. The delay lifetimes versus current density are summarized in Figure 5a. Delay fluorescence from TADF of three exciplex-based OLEDs can be observed without the indication of prompt components. Since the EL emission of exciplex-based OLEDs totally originates from the delay fluorescence, the greater exciton contribution from ^{3}CT state together with efficient rISC would benefit to device performances of carboline-based exciplex OLEDs. As the driving voltages increases, the delay fluorescence lifetimes for three exciplex-based OLEDs decrease. As more carriers are injected into the emitting layer, triplet-polaron quenching (TPQ) becomes more severe, leading to the decreased device efficiencies. The decrement of delay lifetimes as a function of current density is more alleviated for β-CPTBF-based device, which is consistent with the observed higher device performances at high luminance and better efficiency roll-off as compared to those of α-CPTBF- and CPTBF-based exciplex OLEDs.

By applying different reverse bias (−1 to −9 V) after the positive pulse (5 V) at $t = 0$ μs in TrEL, delay fluorescence lifetimes for three exciplex-based OLEDs decrease as shown in Figure 5b–d. The carrier spikes also appear around $t = 0$–7 μs with different intensity shown in the inset of Figure 5a–c. These carrier spikes resulted from the recombination of de-trapped charges, and the reverse bias accelerates the de-trapping process.[31] With the higher spike intensity shown in TrEL that indicates more trapped carriers inside the device, without forming exciplex at the interface, is the main reason for the formation of excess polaron. α-CPTBF- and CPTBF-based OLEDs show larger turn-off spikes starting at $t = 0$ μs as compared to that of β-CPTBF-based OLED. This result indicates that better charge balance together with less polaron remains in the emitting layer for β-CPTBF-based OLED, which can reduce the possibility of TPQ.

3 | EXPERIMENTAL

Pattern ITO electrode on glass substrates was treated by O_2 plasma (PDC-32G) and sent into a thermal evaporator for layer deposition. All the organic and metal layers were deposited under high vacuum 3×10^{-6} Torr and the

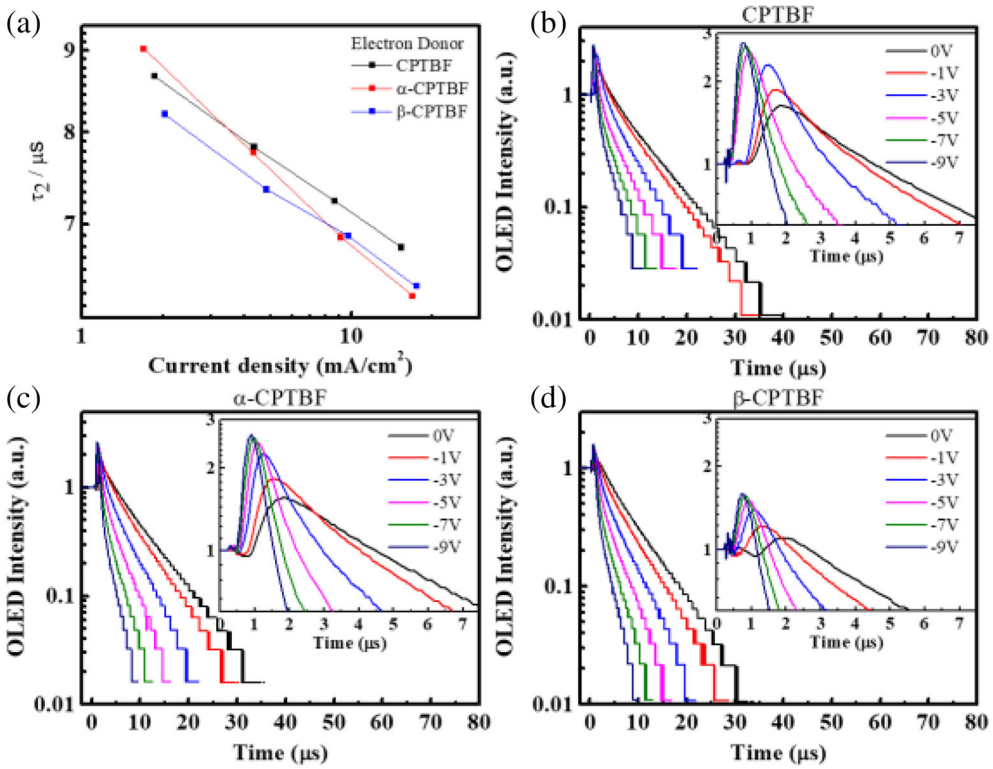

FIGURE 5 (a) Delay lifetimes versus different current density. Time-resolved electroluminescence (TrEL) of exciplex-based OLEDs with (b) CPTBF, (c) α-CPTBF, and (d) β-CPTBF as D at 5 V and the electrical pulse was turned off under different reversed bias. Inset of (b) – (d) shows the zoom-in TrEL at 0–7 μs

devices were transferred into a glove box with N_2 environment and encapsulated under UV radiation. All the materials were deposited by thermal evaporator and the thickness, deposition rates were precisely monitored and controlled by MAXTEK thickness monitor (TM350/400), which uses a quartz crystal as the basic transducing element. By monitoring two evaporating materials with two separated MAXTEK channels, the deposition rate and volume ratio of mixed film can be exactly controlled and obtained with the thickness inaccuracy of 0.5%. Performances of OLEDs, including current density–luminance–voltage characteristics, external quantum efficiency, power efficiency, and EL spectra with CIE coordinate were measured by a spectrometer (Minolta CS-1000) under electrical driving (Keithley 2400). The photophysics of neat and mixed films including absorption spectrum and PL emission were measured by Hitachi U-4100 UV–Vis–NIR and Hitachi 4500, respectively. The setup for time-resolved PL consisted of a 375 nm picosecond laser (LDH-C-375) and monochromator (Horiba, iHR320) while the sample signals were collected by a photomultiplier tube. PL quantum yield values can be achieved by replacing the sample mounts of time-resolved PL into integrating sphere (Quanta-φ manual Rev C F-3029). The setup for time-resolved EL consisted of a function generator (Agilent 33500B), Keithley 2400, photomultiplier (Hamamatsu H6780-20), and oscilloscope (Tektronix TDS2004C). The pulse frequency was 1 kHz and the pulse width was 100 μs (duty ratio 10%).

4 | CONCLUSIONS

Two novel carboline-based hole-transporting materials (α-CPTBF and β-CPTBF) were developed as electron donors for combining a triazine-cored acceptor 3,4-CN to give exciplex-forming systems. The replacement of carbazole in the model molecule (CPTBF) with carboline leads to a new material with deeper HOMO and LUMO energy levels, resulting in hypsochromic shift of PL and EL exciplex emission. The exciplex formations of α-CPTBF:3,4-CN and β-CPTBF:3,4-CN blends have been verified with the significantly red-shifted emissions different from those of constituent donor and acceptor together with the delayed fluorescent observed by time-resolved PL decay experiments. α-CPTBF:3,4-CN and β-CPTBF:3,4-CN blends were adopted as the EML for giving exciplex-based OLEDs with maximum EQE of 7.57 and 7.34%, respectively, which is higher than the model CPTBF:3,4-CN blend (EQE = 6.87%). In addition, the obtained EL λ_{max} based on the new exciplex forming system is blue-shifted as compared to that of the model counterpart due to the deeper HOMO. The superior characteristics can be attributed to the higher PLQY resulting from the higher contribution of delay component on the overall exciplex emission. More importantly, the OLED device based on β-CPTBF:3,4-CN exciplex blend exhibits limited efficiency roll-off at higher luminesce due to more charge balance and less TPQ in the emitting layer concluded from transient EL analysis.

ACKNOWLEDGMENTS

This work was supported by the Ministry of Science and Technology (MOST), Taiwan, under Grants MOST 109-2622-E-155-014, 108-2221-E-155-051-MY3, 107-2221-E-155-058-MY3, 107-2113-M-002-019-MY3; The MEGA project, which has received funding from the European Union's Horizon 2020 research and innovation programme under the Marie Skłodowska-Curie grant agreement No 823720 and academia industry collaboration project under number 1909059.

REFERENCES

[1] J.-H. Lee, C.-H. Chen, P.-H. Lee, H.-Y. Lin, M.-K. Leung, T.-L. Chiu, C.-F. Lin, *J. Mater. Chem. C* **2019**, *7*(20), 5874.
[2] I. Yirang, B. S. Yong, K. J. Han, L. D. Ryun, O. C. Seok, Y. K. Soo, L. J. Yeob, *Adv. Funct. Mater.* **2017**, *27*(13), 1603007.
[3] M. A. Baldo, D. F. O'Brien, Y. You, A. Shoustikov, S. Sibley, M. E. Thompson, S. R. Forrest, *Nature* **1998**, *395*, 151.
[4] H. Uoyama, K. Goushi, K. Shizu, H. Nomura, C. Adachi, *Nature* **2012**, *492*, 234.
[5] L. Bergmann, G. J. Hedley, T. Baumann, S. Bräse, I. D. W. Samuel, *Sci. Adv.* **2016**, *2*(1), e1500889.
[6] X. Cai, X. Li, G. Xie, Z. He, K. Gao, K. Liu, D. Chen, Y. Cao, S.-J. Su, *Chem. Sci.* **2016**, *7*, 4264.
[7] T.-A. Lin, T. Chatterjee, W.-L. Tsai, W.-K. Lee, M.-J. Wu, M. Jiao, K.-C. Pan, C.-L. Yi, C.-L. Chung, K.-T. Wong, C.-C. Wu, *Adv. Mater.* **2016**, *28*(32), 6976.
[8] T. Zhang, B. Chu, W. Li, Z. Su, Q. M. Peng, B. Zhao, Y. Luo, F. Jin, X. Yan, Y. Gao, H. Wu, F. Zhang, D. Fan, J. Wang, *ACS Appl. Mater. Interfaces* **2014**, *6*(15), 11907.
[9] H. Nakanotani, T. Furukawa, K. Morimoto, C. Adachi, *Sci. Adv.* **2016**, *2*, 1.
[10] P. Deotare, W. Chang, E. Hontz, D. Congreve, L. Shi, P. Reusswig, B. Modtland, M. Bahlke, C. Lee, A. Willard, *Nat. Mater.* **2015**, *14*(11), 1130.
[11] K. Goushi, K. Yoshida, K. Sato, C. Adachi, *Nat. Photonics* **2012**, *6*(4), 253.
[12] D. Graves, V. Jankus, F. B. Dias, A. P. Monkman, *Adv. Funct. Mater.* **2014**, *24*(16), 2343.
[13] P. Yuan, X. Guo, X. Qiao, D. Yan, D. Ma, *Adv. Opt. Mater.* **2019**, *7*, 1801648.
[14] B. Zhao, H. Zhang, Y. Miao, Z. Wang, L. Gao, H. Wang, Y. Hao, B. Xu, W. Li, *J. Mater. Chem. C* **2017**, *5*(46), 12182.
[15] Y.-S. Park, S. Lee, K.-H. Kim, S.-Y. Kim, J.-H. Lee, J.-J. Kim, *Adv. Funct. Mater.* **2013**, *23*(39), 4914.
[16] Y. Tao, Q. Wang, C. Yang, Q. Wang, Z. Zhang, T. Zou, J. Qin, D. Ma, *Angew. Chem. Int. Ed.* **2008**, *47*(42), 8104.
[17] J. S. Moon, D. H. Ahn, S. W. Kim, S. Y. Lee, J. Y. Lee, J. H. Kwon, *RSC Adv.* **2018**, *8*(31), 17025.

[18] J.-W. Jun, K.-M. Lee, O. Y. Kim, J. Y. Lee, S.-H. Hwang, *Synth. Met.* **2016**, *213*, 7.
[19] S. Gong, Y. Chen, J. Luo, C. Yang, C. Zhong, J. Qin, D. Ma, *Adv. Funct. Mater.* **2011**, *21*(6), 1168.
[20] S. H. Jeong, C. W. Seo, J. Y. Lee, N. S. Cho, J. K. Kim, J. H. Yang, *Chem.Asian J.* **2011**, *6*(11), 2895.
[21] Y. Im, J. Y. Lee, *Chem. Commun.* **2013**, *49*, 5948.
[22] C. W. Lee, Y. Im, J.-A. Seo, J. Y. Lee, *Chem. Commun.* **2013**, *49*, 9860.
[23] M. Takao, S. Hisahiro, S. Yuki, T. Jun-ichi, K. Junji, *Chem. Lett.* **2011**, *40*, 306.
[24] Q. Wu, M. Wang, X. Cao, D. Zhang, N. Sun, S. Wan, Y. Tao, *J. Mater. Chem. C* **2018**, *6*, 8784.
[25] W.-Y. Hung, T.-C. Wang, P.-Y. Chiang, B.-J. Peng, K.-T. Wong, *ACS Appl. Mater. Interfaces* **2017**, *9*, 7355.
[26] W. Li, J. Qiao, L. Duan, L. Wang, Y. Qiu, *Tetrahedron* **2007**, *63*, 10161.
[27] T. C. Lin, M. Sarma, Y. T. Chen, S. H. Liu, K. T. Lin, P. Y. Chiang, W. T. Chuang, Y. C. Liu, H. F. Hsu, W. Y. Hung, K. T. Wong, *Nat. Commun.* **2018**, *9*(1), 1.
[28] H.-F. Chen, T.-C. Wang, S.-W. Lin, W.-Y. Hung, H.-C. Dai, H.-C. Chiu, K.-T. Wong, M.-H. Ho, T.-Y. Cho, C.-W. Chen, C.-C. Lee, *J. Mater. Chem.* **2012**, *22*, 15620.
[29] W.-Y. Hung, P.-Y. Chiang, S.-W. Lin, W.-C. Tang, Y.-T. Chen, S.-H. Liu, P.-T. Chou, Y.-T. Hung, K.-T. Wong, *ACS Appl. Mater. Interfaces* **2016**, *8*, 4811.
[30] H. Shin, J. H. Lee, C. K. Moon, J.-S. Huh, B. Sim, J.-J. Kim, *Adv. Mater.* **2016**, *28*, 4920.
[31] Z. D. Popovic, H. Aziz, *J. Appl. Phys.* **2005**, *98*(1), 013510.

SUPPORTING INFORMATION

Additional supporting information may be found online in the Supporting Information section at the end of this article.

How to cite this article: Chen C-H, Cheng J-T, Ding W-C, et al. New carboline-based donors for green exciplex-forming systems. *J Chin Chem Soc*. 2021;68:482–490. https://doi.org/10.1002/jccs.202000456